

8(c). Flume experiments on the durability of sandy microbial mat fragments during transport

Juergen Schieber

It is widely understood that benthic microbes impart a considerable increase in erosion resistance to the substrate by acting as a binding matrix between sediment grains (Neumann et al., 1970). The interplay of sedimentation processes, environmental parameters, and microbial responses produces a wide array of sedimentary features that are increasingly recognized in the rock record and aid in putting the microbial contribution to sediment surface dynamics into proper perspective (e.g. Schieber, 2004). When eroded, either wholly or partially, microbial mat fragments also form sedimentary particles with unique properties (physical and chemical) and responses (biological) to external stimuli.

Whereas the parameters that are associated with microbial mat erosion, such as cohesiveness, current strength, and prior history, are at least known in their magnitude from several case studies (e.g. Neumann et al., 1970; Yallop et al., 1994; Paterson et al., 1994; Paterson, 1997), little direct observational data exist that document what happens to microbial mat fragments during transport. Basic questions of interest to the sedimentologist are for example the survivability of mat fragments over the course of transport, as well as their transport modifications and eventual destruction or burial.

Study materials

In the study presented here, microbial mat fragments from a natural occurrence of a cyanobacterial mat (Fig. 8(c)-1A) were studied in a sand-filled racetrack flume (Fig. 8(c)-1B, -1C, -1D) in order to arrive at estimates of likely transport distance prior to complete mat destruction. Desiccated fragments of the mat shown in Fig. 8(c)-1A were collected for the experiment. Half of the fragments were kept moistened for one week prior to the flume run to allow the mat to revitalize.

Examination of the desiccated starting material under the SEM shows a top to bottom decline in visible microbial filaments and a corresponding increase in mineral matter (Fig. 8(c)-2A). Identifiable microbial filaments only occur in the top portion of the mat (Fig. 8(c)-2B and -2C), whereas further down (Fig. 8(c)-2D, -2E, -2F) filaments become less conspicuous and the connective matter between mineral grains is largely extracellular polymer substance (EPS). The mat surface consists mainly of tangled microbial filaments set in a matrix of EPS (Fig. 8(c)-2G through -2K). The EPS matrix gives the surface a “smoothed” appearance (Fig. 8(c)-2I, -2J).

Macroscopically, the dried mat fragments consist of a mixture of organic debris and mineral grains in a microbial matrix and have curved up edges (Fig. 8(c)-3A, -3B). They are of grey-brownish appearance after several days of desiccation (Fig. 8(c)-3A) due to bleaching of cyanobacterial pigments in sunlight. The mat may still appear green if freshly desiccated or if dried away from sunlight (Fig. 8(c)-3B). Closer inspection shows that most fragments contain narrow desiccation-related cracks (Fig. 8(c)-3A, -3B) that predetermine future fragmentation.

Observations from flume runs with desiccated mat fragments

Initial flume runs were conducted at various flow velocities (40 to 70 cm/sec, measured mid-channel at half depth) and at a flow depth of 8 centimetres. The sand surface was rippled (lower flow regime) across the entire velocity range. At low velocities (40 to 50 cm/sec), after being added to the flow, desiccated curved fragments (5 to 8 cm in size) tumbled a metre or two across the flume bottom before locking into the sand with their curved edges (convex up orientation, Fig. 8(c)-3C). Hydration and softening of the fragment, in combination with continued flow, then induced “shedding” of particles from the exposed “back side” of the mat fragment (Fig. 8(c)-3C). For sustained transport, higher flow velocities (60-70 cm/sec) were needed. At such velocities fragments crept over the surface and were picked up by the current intermittently before settling to the surface again. Within 15 minutes the larger fragments (5 to 10 cm across) broke up into smaller pieces because of pre-existing fractures (Fig. 8(c)-3A, -3B). These smaller fragments (2-4 cm in size) readily “fit” into ripple troughs and were buried rapidly by migrating ripples (Fig. 8(c)-3E, -3F). Because net sedimentation was zero in these experiments, fragments could move again once the ripple had migrated down-current. In a situation of net sedimentation, on the other hand, they would not be remobilized. As fragments continued to travel, they continuously lost adherent sediment grains (Fig. 8(c)-3C) and the lower, poorly bound part of the mat (Fig. 8(c)-2) was largely lost within an hour of immersion. The original mat chips slimmed down to thin leathery “skins” of 1-2 mm thickness (Fig. 8(c)-3D) that now traveled much easier and were quite durable. This shedding of adherent sediment grains occurs for both desiccated (“dry”) and revitalized moist (“live”) mat fragments. Whereas large fragments (5 cm’s or more) were dragged and rolled over the bed surface, small centimetre-size fragments tended to travel in bounces and hops and were in suspension for considerable portions of the transport path.

In an extended flume run, starting with eight fragments measuring 5-10 cm across (Fig. 8(c)-3A, -3B), fragments were collected with a 2 mm mesh screen several times during the run, for examination of size reduction (Fig. 8(c)-3). After approximately one hour, the largest remaining fragments measured less than 5 cm across (Fig. 8(c)-3G), and a significant portion (~75%) of the mat material had disintegrated into particles of a few millimeters in size that tended to become buried in the sand substrate (Fig. 8(c)-4F, G) or traveled in suspension and passed through the screen. Approximately twelve hours later the largest remaining fragments typically were less than 3 cm in size (Fig. 8(c)-3H), and between 80-85% of the original material had disaggregated into mm-size or smaller particles. After another twelve hours the largest recoverable fragments measured a mere 1 and 2 cm across, and approximately 95% of the original material had disaggregated (Fig. 8(c)-3I). At a flow velocity between 60-70 cm/sec, mat fragments as pictured in Figure 8(c)-3G, -3H, -3I take, on average, 1 minute or less to cover the 25 m roundtrip through the flume. Thus, at the 25 hour mark the average fragment had traveled a distance equivalent to 35 to 50 kilometers of transport.

Observations from flume runs with “live” mat fragments

Moistened and revitalized mat fragments felt soft and pliable and the originally dried out mat surface had returned to a vibrant dark green color. Mat disintegration over the first 24 hours of

transport is visibly reduced (Fig. 8(c)-4) in comparison with “dry” mat fragments. While there was a general increase in the number of fragments, most of the fragmentation occurred in the first 12 hours of the run (Fig. 8(c)-4D). Even after 12 hours several fragments still measured more than 5 cm across, and fragment #1 still measured 5 centimetres after 24 hours of transport (see Fig. 8(c)-4E). Between 12 and 24 hours, neither fragment size nor fragment numbers changed substantially (Fig. 8(c)-4D, -4E). There was an initial loss of about 25% of mat material due to disintegration into mm-size or smaller particles over the first 6 hours of the experiment. Loss was minor or negligible over the following 18 hours of the experiment. The edges of fragments were ragged initially (Fig. 8(c)-4A), but became quite smooth within the first 6 hours of the experiment (Fig. 8(c)-4C).

Differences between “dry” (desiccated) and “live” (moistened) mat fragments

Comparing the results from the two flume runs (Figs. 8(c)-3 and -4), it is quite clear that “live” mat fragments survive transport much better than “dry” fragments from the same mat. Considering the excellent survival of “live” mat fragments that were still several centimetres in size over 24 hours (Fig. 8(c)-4) of transport, it is likely that these fragments would have been transported for another day or two without significant further degradation.

In both experiments, fragment size-decrease is most notable in the first 12 hours of transport. This probably reflects the fact that small fragments are more likely to travel in suspension, especially if they have lost most of their original mineral ballast. The density of the fragments is then only slightly larger than that of water, and even if they interact intermittently with the sand surface the impact forces are minor. However, whereas there was not much further reduction of fragment size after 12 hours in the case of “live” mat material, fragment size continued to decrease in the case of “dry” mat material, albeit more slowly than in the first 12 hours of the run.

Microscopic examination of mat fragments that were collected after the termination of the respective flume runs shows clearly that a biologically active mat surface is the reason for the observed differences in mat fragment behaviour. Both “live” and “dry” mat fragments were only approximately 1 mm thick (Figs. 8(c)-5A and -6A) because most of the mineral grains of the lower portions of the mat (Fig. 2A) had been lost due to transport. The major difference between the two types of mat material was the presence of a tangled felt of active *Oscillatoria* spp. filaments at the surface of “live” mat material (Fig. 8(c)-6), and the absence thereof in the case of “dry” mat material (Fig. 8(c)-5). The surface of the latter was instead covered with a rehydrated film of EPS that contained old microbial filaments (Fig. 8(c)-5B). The only viable *Oscillatoria* spp. filaments were found in the interior, protected by a thick cover of EPS (Fig. 8(c)-5A). The surfaces of “live” and “dry” mats also differ in two other aspects. First, there is clear evidence of adhesion of new detrital material to the surface of “live” mat fragments (Fig. 8(c)-6A, -6B). The sand in the flume was fine, well sorted quartz sand, whereas the detrital material attached to the original mat fragments was coarse, poorly sorted, and polymineralic (quartz and carbonate grains). Fig. 8(c)-6A shows the addition of a layer of fine quartz grains at the surface of transported “live” mat that is not observed on the surface of transported “dry” mat (Fig. 8(c)-5A). This difference can readily be attributed to the stickiness of freshly produced EPS and the upward growth of *Oscillatoria* spp. filaments (Fig. 8(c)-6C, -6D, -6E) in “live” mat. Secondly,

by comparison with untransported “dry” mat (Fig. 8(c)-2I, -2J), SEM images of the surface of transported “dry” mat show that the surface has been roughened and that variably eroded old microbial filaments are now present at the surface. These features are best explained by abrasion of the EPS surface layer while the fragment traveled over the sandy flume bottom.

Implications for the rock record

There are several implications from these experiments for the interpretation of the sedimentary rock record. For example, physical diminution of eroded microbial mats during transport will produce abundant mm-sized particles that are buried in associated sands (Fig. 8(c)-4F, -4G). However, erosion and transport of desiccated “dry” mat fragments is likely to produce a much larger proportion of small (mm-sized) mat debris than erosion and transport of fresh “live” mat fragments.

Finding large curved fragments (5 cm or larger) of “dry” mat buried in sandy sediments probably indicates burial shortly after onset of transport (probably within an hour) and close to their point of origin (a few kilometers at best). These time and distance constraints should be considered maximum estimates because in actual sedimentary systems erosion and transport is episodic, and typically related to short-lived erosive events (floods, storms, etc.) followed by deposition due to decreasing wave action and/or current flow (e.g. Reineck and Singh, 1980). Thus, unlike in our flume experiments, net deposition is likely to prevail after initial erosion, and burial of a mat fragment will occur earlier in transport history and closer to its point of origin.

Finding significant amounts of cm-size “dry” mat debris in an ancient sandstone should probably be taken as an indication that the source of this material was at best no further than a day’s travel or 30-50 kilometers away, and quite probably originated closer. In contrast, the “self-repair” potential of “live” mats can potentially allow cm-size fragments to travel for multiple days and distances of the order of hundreds of kilometers. This effect could be significant in a setting with very small net sedimentation rates, and would be negligible in cases of high net sedimentation. In the latter case, because of rapid burial of mat fragments (Figs. 8(c)-3E and -3F) there should not be much difference from the travel time and distance estimated for “dry” mat material.

The thickness of microbial mats that grow on sandy substrates can be in excess of a centimetre when a fresh mat is examined (e.g. Gerdes and Krumbein, 1987), but in the illustrated experiments only the topmost layer with abundant EPS and microbial filaments (Fig. 8(c)-2A) showed a high degree of cohesiveness during transport experiments. Whereas one can sample a cm-thick mat because bacterial mucilage holds together the lower portions of the mat, during transport, this portion disintegrates rapidly and leaves mainly a leathery membrane of 1-2 mm thickness (Fig. 8(c)-3E). Thus, mat fragments that have been transported for more than a short distance (less than 1 km) are likely reduced to thin sheets. Conversely, if we find thick (5 to 10 mm) microbial sand chips in the rock record (cf. Pflüger and Gresse, 1996) it can probably be taken as an indication that they were transported for a short distance only.

One should point out in this context that the types of cyanobacteria that dominate a given mat can exert an influence on the transport behaviour. For example, in mats dominated by *Lyngbia* spp. or *Microcoleus chthonoplastes*, the highly cohesive surface layer with felted filaments may

be as much as 10 mm deep (G. Gerdes, pers. com., 2006). Consequently, such mats may be able to retain their initial thickness for greater transport distances than the observed *Oscillatoria* spp. mats. No experimental work with such strongly felted mat fragments has been conducted to date.

Summary

The above discussion indicates that it can make a difference to our conclusions whether a mat fragment was eroded from a dried out mat, or from a biologically active (“live”) mat. It is therefore desirable to distinguish between the two mat fragment types when analyzing the rock record. Presence of curved fragments can probably be taken as a good indication of a desiccated mat source, whereas signs of soft deformation, such as large (5 to 10 cm across) mat fragments that show roll-ups or fold-overs (Simonson and Carney, 1999; Schieber, 1999) would suggest that the fragments were more likely eroded from a “live” mat.

By contrasting “live”, photosynthetically active mat fragments with desiccated fragments from the same occurrence, flume experiments allowed a determination of the geological significance of active microbial surface binding on the durability of microbial mat fragments in a sandy depositional system. Both types of mat material undergo an initial rapid reduction of size. Size degradation slows down once the population of mat fragments largely consists of centimetre-size fragments and transport is mainly in suspension instead of as bedload. However, whereas the size of “live” fragments stabilizes at that point, “dry” mat fragments suffer continued size reduction due to abrasion. Desiccated mat fragments behave in a brittle fashion during initial transport, break down into smaller fragments than the flexible “live” fragments, and show evidence of surface abrasion of the dried organic matrix. Under conditions of significant net sedimentation and lower flow regime (ripples) many mat fragments are likely to be buried by migrating ripples early in transport history, close to their point of origin.

Unless strongly felted, microbial mat fragments will tend to lose most of their attached ballast of sediment grains early in transport history and turn into thin leathery films of one to two millimeter thickness within an hour. Thus, under upper flow regime conditions all but the largest of these fragments will travel in suspension due to the small density contrast between mat fragments and water, and may therefore travel considerable distances.

Figures and Captions: Chapter 8(c)

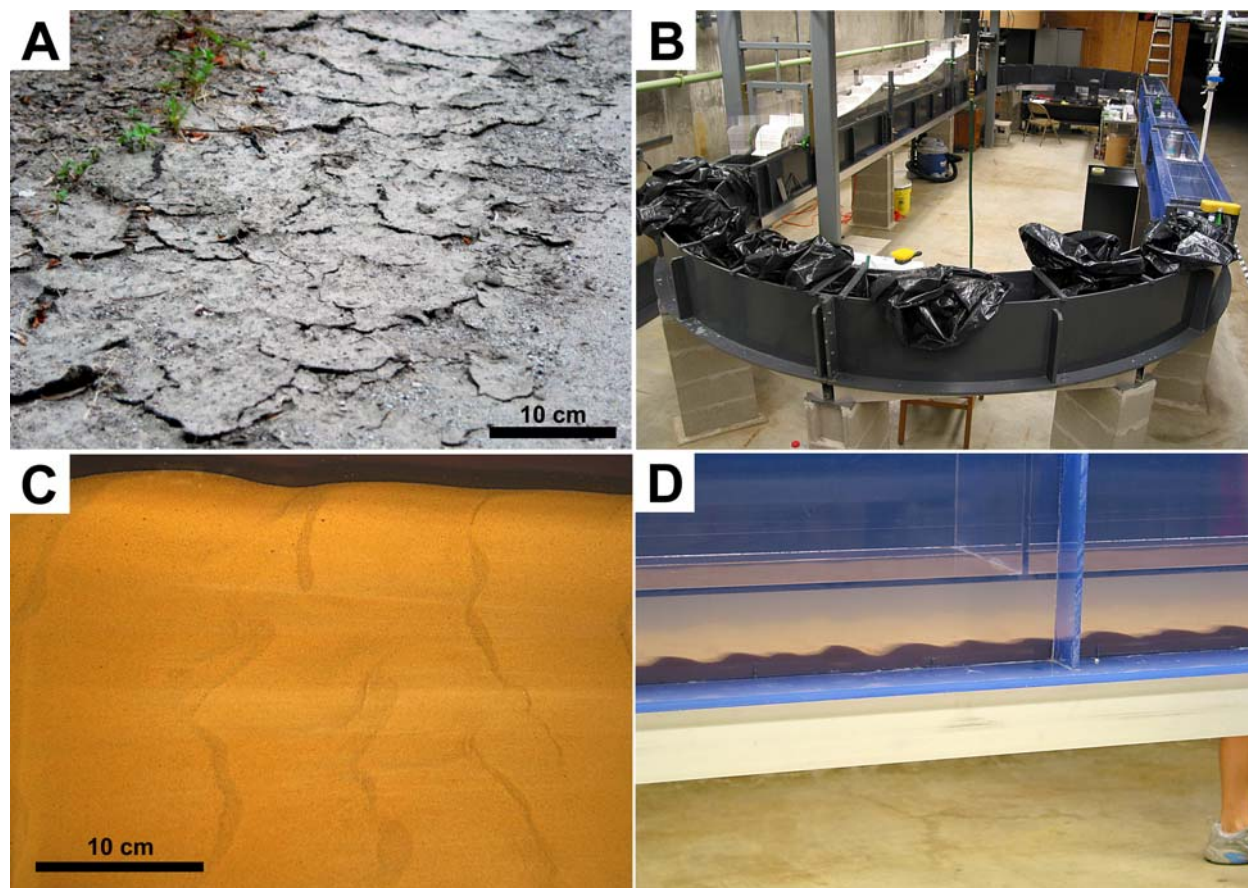
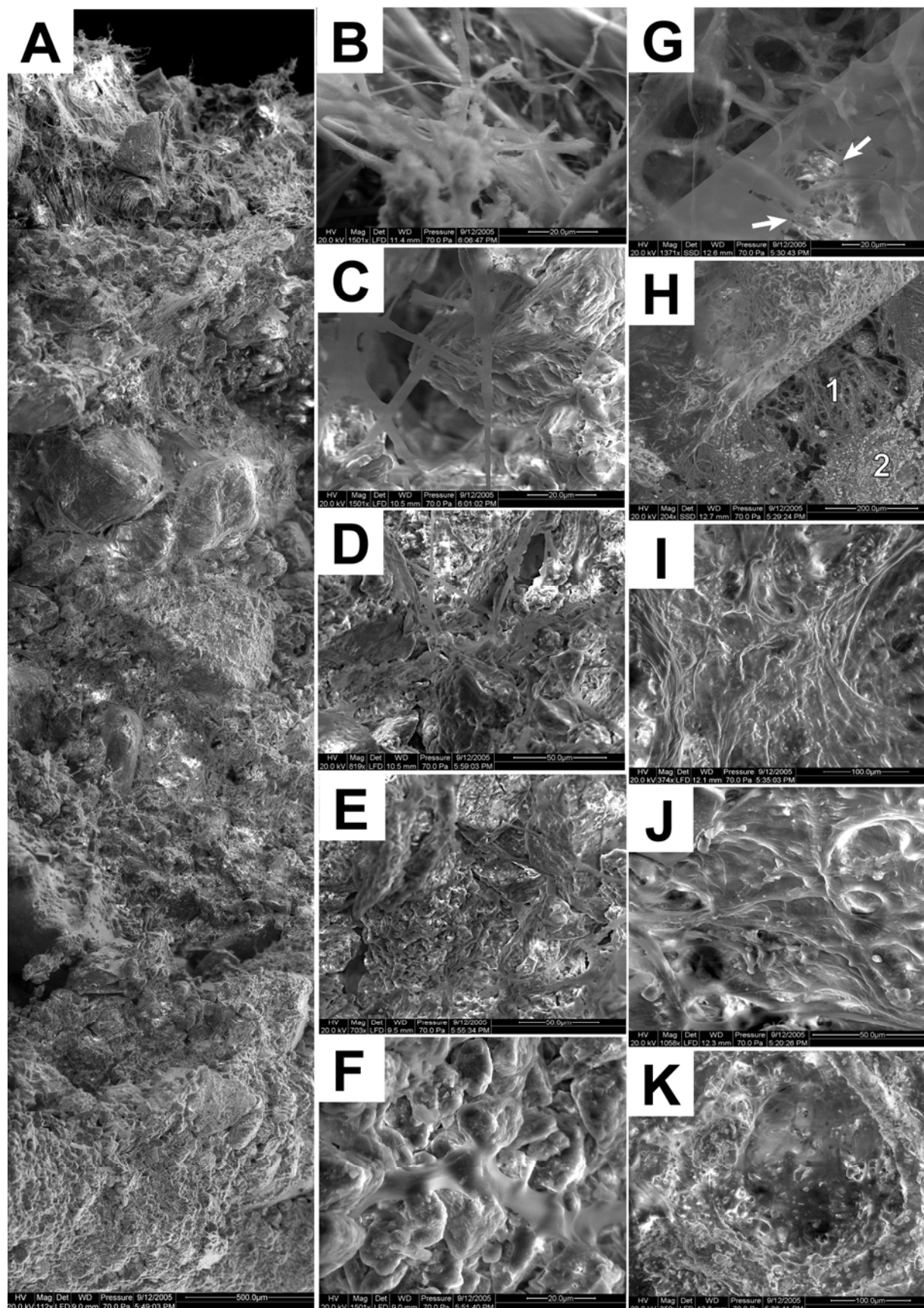


Fig. 8(c)-1: (A) The raw material, desiccation-cracked cyanobacterial (*Oscillatoria* spp.) mats on a sandy substrate from a roadside ditch. (B) The racetrack flume at the Shale Research Laboratory of Indiana University. The flume has an 11.5x3.25m footprint and the water is moved with a paddle belt (left side of flume). This method of propulsion minimizes the shredding and disintegration of cohesive particles, such as clay flocs and microbially bound materials. (C and D) The sand bed on which the experiments were conducted: (C) plan view of migrating current ripples (10-15 cm wavelength); (D) side view of rippled sand bed.



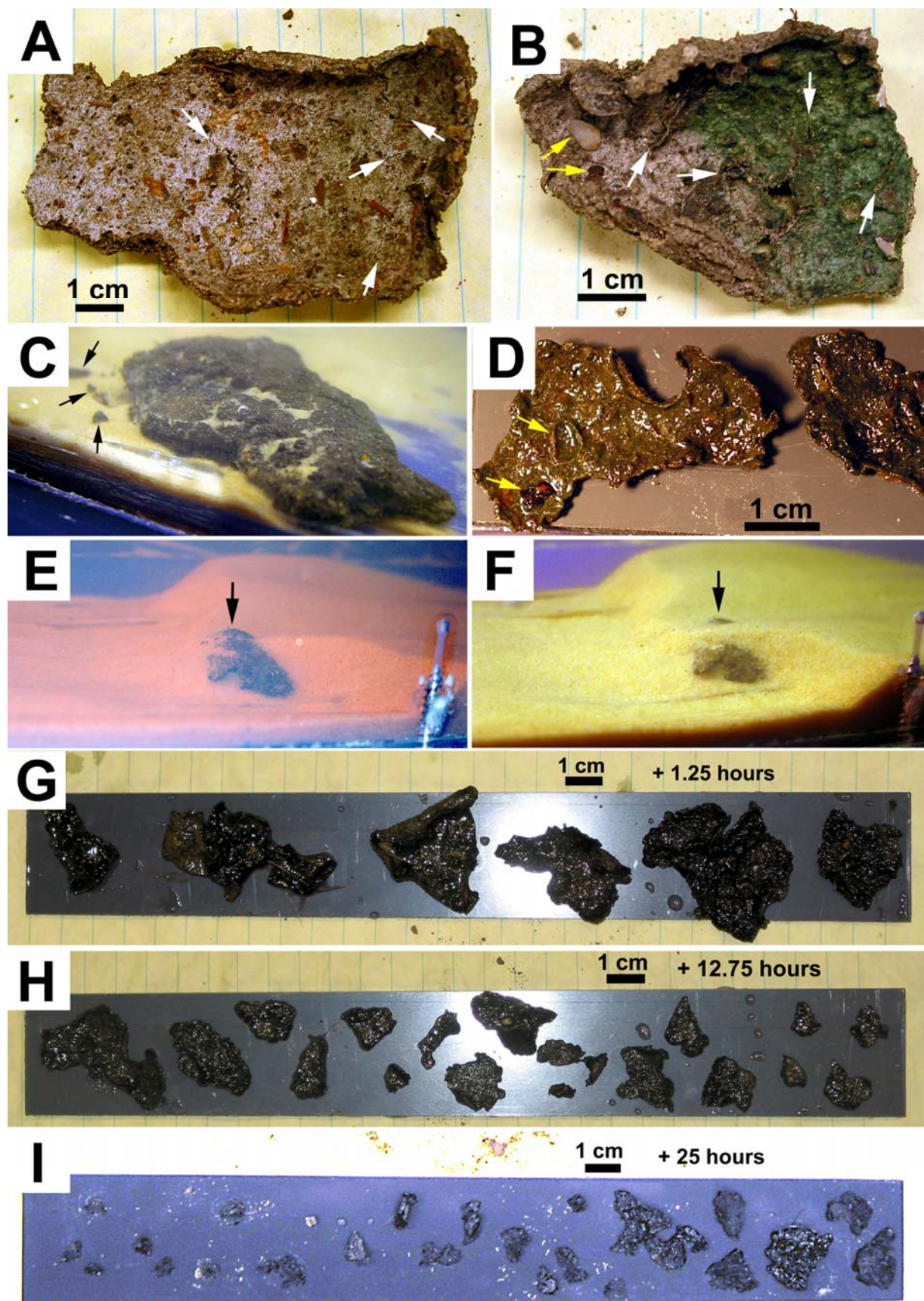
In: *Atlas of microbial mat features preserved within the clastic rock record*, Schieber, J., Bose, P.K., Eriksson, P.G., Banerjee, S., Sarkar, S., Altermann, W., and Catuneau, O., (Eds.), Elsevier, p. 248-257. (2007)

Fig. 8(c)-2: A collection of SEM images of a dried piece of microbial mat (see Fig. 8(c)-1A):

(A) Mosaic of low magnification SEM images across the entire thickness of a dried mat sample (total thickness ~ 5 mm). The image shows a general downward decline in visible microbial filaments and a corresponding increase in mineral matter (quartz, carbonate particles, clay).

The images in the middle row (B through F) are higher magnification images from the cross-section shown in (A) and are arranged top to bottom. (B) At the very top of the mat we see abundant dried filaments of *Oscillatoria* spp. and little mineral matter. (C) Somewhat below we see a meshwork of dried filaments that surround and hold together mineral grains, but there is still abundant pore space. (D and E) Further down into the mat the filaments are less conspicuous, porosity has decreased, and there is connecting matter between and on grains that is of variable morphology and which represents a mixture of dried filaments and extracellular polymer substance (EPS). (F) A close-up of a dried out strand of EPS that connects detrital grains.

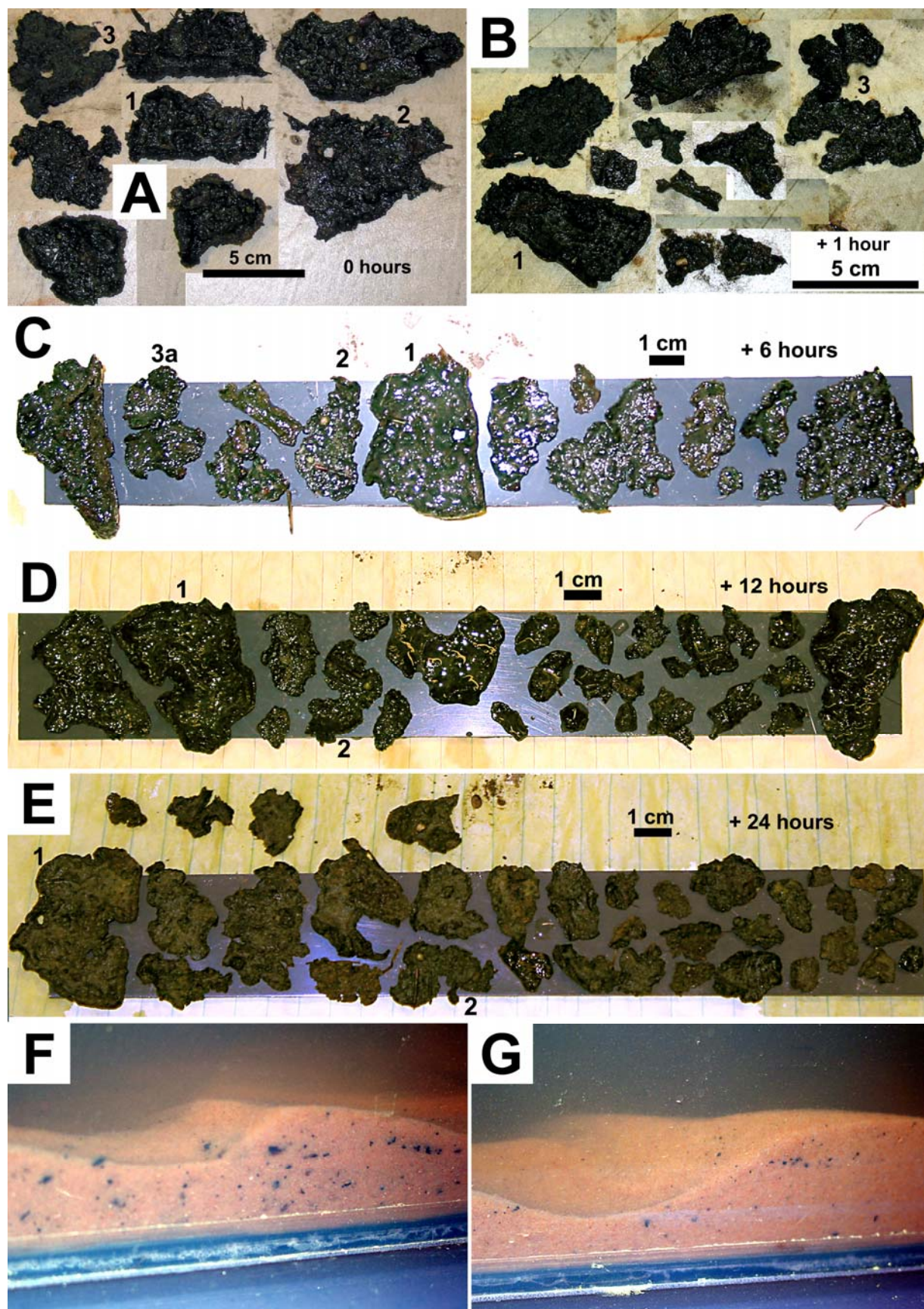
The images in the right row (G through K) are SEM photos of the mat surface. (G) Split backscatter (upper left) and secondary electron image of mat surface. The secondary electron image shows mainly surface topography which is smoothed by a film of dried out EPS. Where the EPS film is disrupted (arrows) we can see into lower layers of the mat. Backscatter electrons image density (lower right) and therefore “see” through the low density EPS surface and show the denser filaments embedded in it. (H) Another split the image, but this time the upper left corner is the secondary electron (SE) image, and the lower right corner is the backscatter (BSE) image. The image demonstrates that although the surface may look more or less uniform in SE, this is mainly due to masking by the surficial EPS film. Beneath the surface (BSE) the mat may be heterogeneous, with some areas dominated by microbial filaments (area 1), and others by mineral matter (area 2). (I and J) Variable magnification SE images of mat surface with *Oscillatoria* spp. filaments and small mineral grains enclosed by dried out EPS matrix. (K) SE image of mat surface with mineral grains adhering to surficial EPS.



In: *Atlas of microbial mat features preserved within the clastic rock record*, Schieber, J., Bose, P.K., Eriksson, P.G., Banerjee, S., Sarkar, S., Altermann, W., and Catuneau, O., (Eds.), Elsevier, p. 248-257. (2007)

Fig. 8(c)-3: Observations from flume run with dried mat fragments:

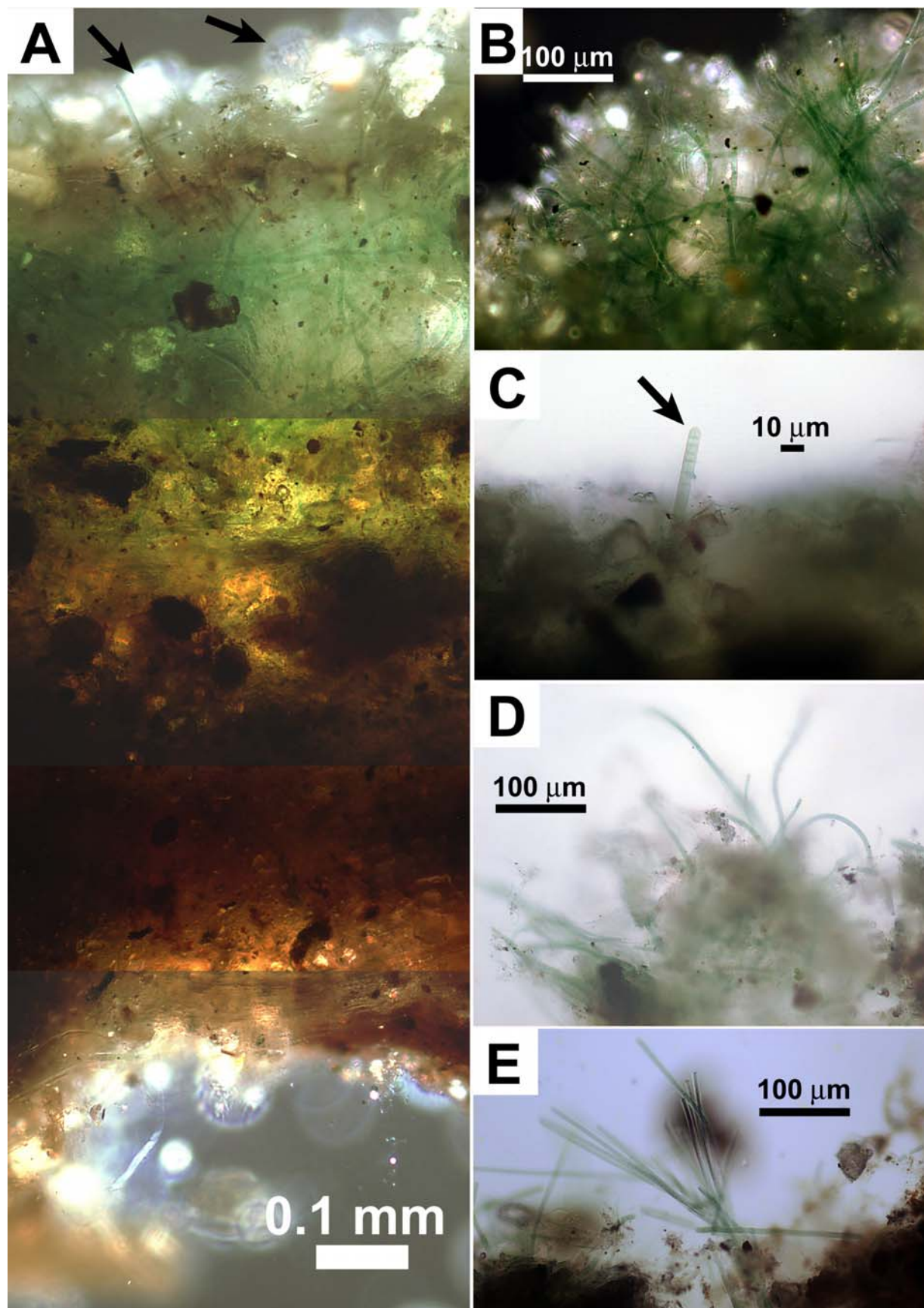
(A and B) Examples of mat fragments. Fragments have curled-up edges and embedded plant particles (brownish) and small pebbles and granules. White arrows point to existing fractures along which initial disintegration will begin. (C) The fragment from (A) has turned convex-up and stopped moving. Note scouring at upstream edge of fragment and breaking off of small pieces due to current drag (black arrows). (D) After one hour the initially 5 mm thick fragments have been reduced to thin (1-2 mm) leathery “skins”. The fragment shown broke off the larger piece in (B) and can be identified because of the mold of a small pebble and a piece of plant matter (yellow arrows in B and D). (E and F) A mat fragment (black arrow) being buried by a migrating ripple. The pictures were taken 1 minute apart. (G) Remaining large fragments after 1.25 hours. (H) Remaining large fragments after 12.75 hours. (I) Remaining recoverable fragments after 25 hours.



In: *Atlas of microbial mat features preserved within the clastic rock record*, Schieber, J., Bose, P.K., Eriksson, P.G., Banerjee, S., Sarkar, S., Altermann, W., and Catuneau, O., (Eds.), Elsevier, p. 248-257. (2007)

Fig. 8(c)-4: Observations from flume run with wet “live” mat fragments:

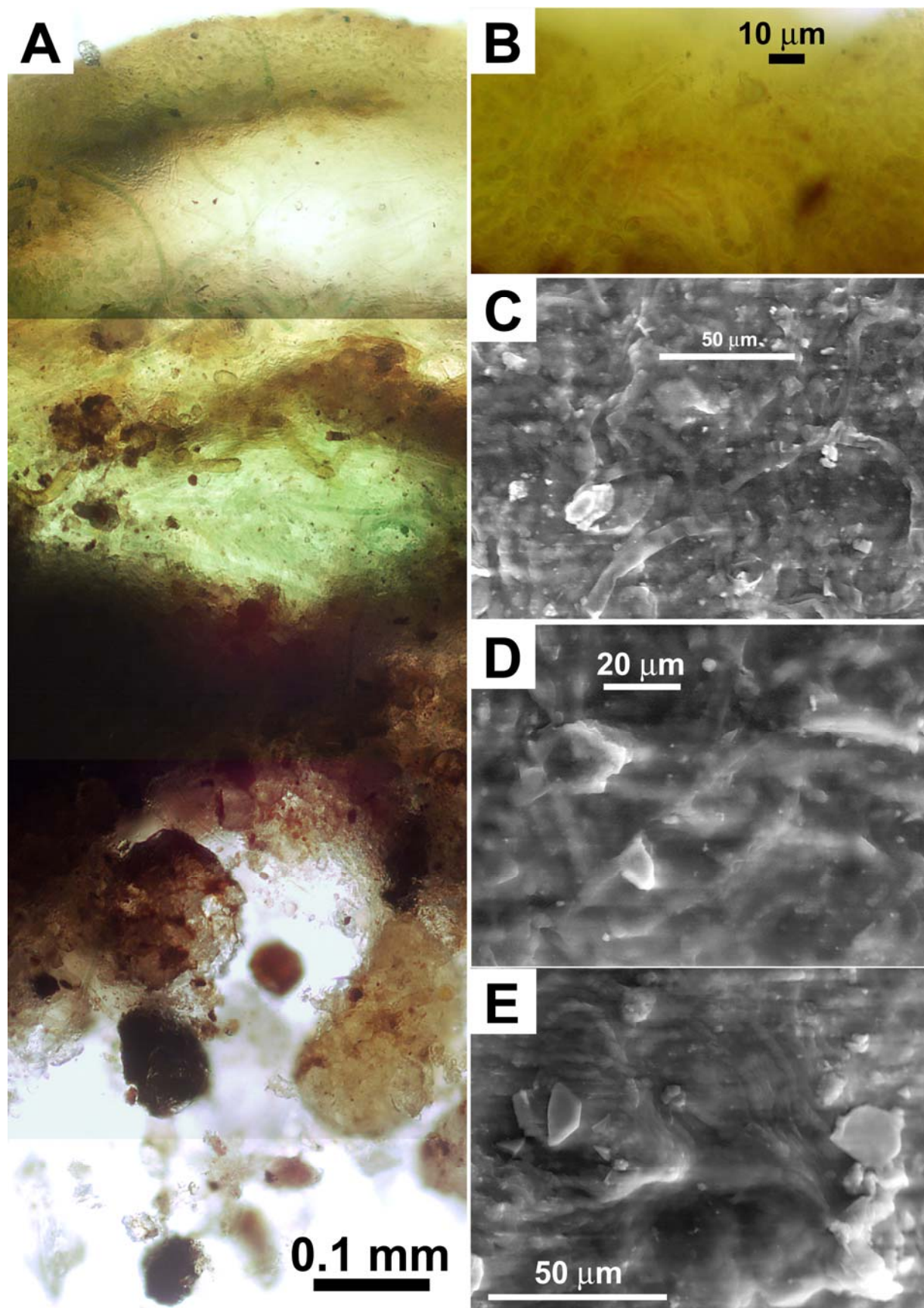
(A) The eight mat fragments that were placed into the flume at the start of the experiment. The fragments are soft and flexible. (B) After one hour several samples are still largely unchanged, whereas others have broken into several pieces of a few cm across. (C) Recovered mat fragments after 6 hours. (D) Recovered mat fragments after 12 hours. (E) Recovered mat fragments after 24 hours. Some fragments with unique shape or components (marked 1 and 2) can be tracked through the course of the experiment. (F and G) Sand bed with ripples and incorporated dark particles that resulted from mat disintegration.



In: *Atlas of microbial mat features preserved within the clastic rock record*, Schieber, J., Bose, P.K., Eriksson, P.G., Banerjee, S., Sarkar, S., Altermann, W., and Catuneau, O., (Eds.), Elsevier, p. 248-257. (2007)

Figure 5: A collection of photomicrographs (visible light) through a “live” mat sample that was retrieved after flume run:

(A) Cross-section through mat that shows a green top portion because of actively growing *Oscillatoria* spp. filaments. The lower, darker, portion of the sample consists of detrital mineral grains held together by dead filaments and EPS. A surficial layer of quartz grains (whitish; black arrows) is attached to the underlying microbial layer (green). This mat sample is much thinner (1.2 mm) than the mat prior to transport (5 mm, Fig. 8(c)-2) because most of the more loosely attached lower sediment (Fig. 8(c)-2) has been lost during transport. (B) Close-up of the actively growing top portion of the mat. *Oscillatoria* spp. filaments are weaving around newly trapped surficial sand grains. (C) Close-up of *Oscillatoria* spp. filament (arrow) that is poking through the quartz grain encrusted surface. (D and E) Bundles of *Oscillatoria* spp. filaments growing at the mat surface.



In: *Atlas of microbial mat features preserved within the clastic rock record*, Schieber, J., Bose, P.K., Eriksson, P.G., Banerjee, S., Sarkar, S., Altermann, W., and Catuneau, O., (Eds.), Elsevier, p. 248-257. (2007)

Fig. 8(c)-6: A collection of photomicrographs (visible light) through a “dry” mat sample that was retrieved after flume run:

(A) Cross-section through mat that shows a yellowish top with some filaments inside. This appears to be mainly rehydrated EPS with embedded dead cyanobacterial filaments. (B) enlargement of this top zone that shows entombed cyanobacterial filaments. Beneath this top layer of EPS, still green filaments (probably *Oscillatoria* spp.) are hidden in the core zone of the fragment. (C through E) SEM images of the mat surface. By comparison with images taken before the flume run (Fig. 8(c)-2), these surfaces are rougher and show exposure and erosion of textural features such as cyanobacterial filaments. These features are due to abrasion of the mat while it traveled over the sandy flume bottom.

References

- Gerdes, G., and Krumbein, W.E., 1987, *Biolaminated Deposits*. Lecture Notes in Earth Sciences 9, Springer, New York, 183 pp.
- Neumann, C.A., Gebelein, C.D., and Scoffin, T.P., 1970, The composition, structure and erodability of subtidal mats, Abaco, Bahamas. *Journal of Sedimentary Petrology*, v. 40, p. 274-297.
- Paterson, D.M., 1997, Biological mediation of sediment erodibility: ecology and physical dynamics. in Burt, N, Parker, R, Watts, J, eds., *Cohesive Sediments*. London, John Wiley and Sons, p. 215 – 229.
- Paterson, D.M., Yallop, M., and George, C., 1994, Stabilization. In: *Biostabilization of Sediments*, W.E. Krumbein, D.M. Paterson, and L.J Stal (Eds.), Bibliotheks und Informationssystem der Universität Oldenburg, Oldenburg, p. 401-432.
- Pflüger, F., and Gresse, P.G., 1996, Microbial sand chips – a non-actualistic sedimentary structure. *Sedimentary Geology*, v. 102, p. 263-274.
- Reineck, H.E., and Singh, I.B., 1980, *Depositional Sedimentary Environments*, Springer-Verlag, Berlin, Heidelberg, New York, 549 pp.
- Simonson, B.M., and Carney, K.E., 1999, Roll-up structures: Evidence of in situ microbial mats in Late Archean deep shelf environments. *Palaios*, v. 14, p. 13–24.
- Schieber, J., 1999, Microbial Mats in Terrigenous Clastics: The Challenge of Identification in the Rock Record. *Palaios*, v. 14, p. 3-12.
- Schieber, J., 2004, Microbial Mats in the Siliciclastic Rock Record: A Summary of Diagnostic Features. In: P.G. Eriksson, W. Altermann, D. Nelson, W.U. Mueller, O. Catuneanu, and K. Strand (editors), *The Precambrian Earth: Tempos and Events, Developments in Precambrian Geology*, Elsevier, p. 663-672.
- Yallop, M.L., De Winder, B., Paterson, D.M., and Stal, L.J., 1994, Comparative study on primary production and biogenic stabilization of cohesive and non-cohesive marine sediments inhabited by microphytobenthos. *Estuarine, Coastal and Shelf Science*, v. 39, p. 565-582.